Energy Conversion and Management 302 (2024) 118160

Contents lists available at ScienceDirect

Energy Conversion and Management

journal homepage: www.elsevier.com/locate/enconman

Techno-economic and environmental analyses of a solar-assisted Stirling engine cogeneration system for different dwelling types in the United Kingdom

Dibyendu Roy [a], Shunmin Zhu [a,b,*], Ruiqi Wang [a], Iker González-Pino [c], María Herrando [b,d], Christos N. Markides [b], Anthony Paul Roskilly [a]

[a] Department of Engineering, Durham University, Durham DH1 3LE, UK
[b] Clean Energy Processes (CEP) Laboratory, Department of Chemical Engineering, Imperial College London, South Kensington Campus, London SW7 2AZ, UK
[c] ENEDI Research Group, Department of Energy Engineering, Faculty of Engineering of Bilbao, University of the Basque Country UPV/EHU, Plaza Torres Quevedo 1, Bilbao 48013, Spain
[d] Instituto Tecnológico de Aragón (ITAINNOVA), Zaragoza 50007, Spain

ARTICLE INFO

Keywords:
Combined heat and power
Stirling engine
Photovoltaic-thermal collector
Technoeconomic analysis
Exergy analysis
Environmental analysis

ABSTRACT

In this study, a hybrid cogeneration system that combines photovoltaic-thermal (PV-T) collectors with a Stirling engine, and a battery-pack-based energy option is proposed for residential applications. The system's purpose is to fulfil the electrical and heating requirements of different types of houses in the United Kingdom, including detached, semi-detached and mid-terraced houses. This study includes a comprehensive assessment of the techno-economic feasibility and environmental impact of the proposed integrated energy system, after determining the appropriate sizing of the system's components for the three different house types. The exergy efficiency of the integrated system for detached houses (with a 1 kWe-Stirling engine plus 28 m^2 of PV-T collector array) is found to be higher compared to that for the semi-detached and mid-terraced house configurations, with the highest efficiency of 22 %. In terms of economic performance, detached houses have the lowest levelized cost of electricity (0.622 £/kWh), levelized cost of heat (0.147 £/kWh), and levelized cost of total energy (0.205 £/kWh). Furthermore, the system demonstrates the maximum potential reduction in CO_2 emissions in detached houses. The achieved CO_2 emissions reduction rates for different house configurations fall within the range of 30 % to 45 %. The proposed hybrid cogeneration system shows promise as an effective and sustainable solution to meet the energy demands of various residential house types in the United Kingdom, offering improved efficiency, cost-effectiveness, and substantial reductions in carbon emissions for detached houses.

1. Introduction

Based on the most recent report [1], it is estimated that natural gas fulfilled approximately 74 % of the heating and domestic hot water (DHW) requirements in buildings across the United Kingdom (UK). Furthermore, the breakdown of direct carbon emissions from buildings reveals that homes contribute around 77 % of emissions, while commercial buildings account for up to 14 %, and public buildings contribute 9 % to the overall emissions [1]. In line with these findings, the UK government introduced the Heat and Buildings Strategy in 2021 aimed at decarbonizing all buildings across the country [2]. This crucial initiative aims to decarbonize all buildings across the country, reflecting their unwavering commitment to achieving net zero emissions by 2050. In this sense, the UK has taken a major step in combating climate change, becoming the first major economy to adopt a legally binding target of achieving net-zero emissions by 2050 [3]. This ambitious commitment sets the stage for a pioneering effort to fully decarbonize not only the power sector but also the heating of homes, buildings, and other critical industries.

In this context, it becomes crucial to enhance the adoption of renewable energy sources to minimize carbon emissions from buildings [4]. Solar-based technologies emerge as a pivotal solution in attaining the net-zero goal by 2050. Among these technologies, solar photovoltaic (PV), solar thermal collector (STC), and solar photovoltaic-thermal (PV-T) stand out as attractive options, directly converting sunlight into

* Corresponding author at: Department of Engineering, Durham University, Durham DH1 3LE, UK.
E-mail address: shunmin.zhu@durham.ac.uk (S. Zhu).

https://doi.org/10.1016/j.enconman.2024.118160
Received 27 October 2023; Received in revised form 12 January 2024; Accepted 29 January 2024
Available online 6 February 2024

Nomenclature

Symbols

A_c	Total aperture area, m^2
ACF_{Yr}	Annual cash flow, £
C_0	Capital cost, £
C_{CO_2}	Unit cost of CO_2, £/t CO_2
$C_{O\&M\&R}$	Annual operational, maintenance, and component replacement costs, £
$C_{TOT,SAV}$	Total cost saving, £
$CPCS$	Total cost savings resulting from the reduction of CO_2 penalties over the lifespan of the system, £
d	Discount rate, %
E	Net annual energy production, Wh or J
$EF_{CO_2,gas}$	CO_2 emission factors for natural gas network, $kgCO_2$-eq/Wh
$EF_{CO_2,grid}$	CO_2 emission factors for grid electricity, $kgCO_2$-eq/Wh
$EM_{CO_2,ref}$	Total CO_2 emissions from the conventional system, $kgCO_2$-eq
ER	Total CO_2 emissions reduction associated with the installation of the proposed system, $kgCO_2$-eq
ERR	CO_2 emissions reduction rate
Ex	Exergy, W
EX_{ELEC}	Electricity sold to grid, Wh or J
i	Rate of inflation, %
I_{tot}	Solar irradiance, W/m^2
IM_{ELEC}	Imported electricity, Wh or J
NG_{ref}	Amount of natural gas consumed by the reference house, Wh or J
q_u	Useful heat flow per meter square, W/m^2
Q	Heat output, W
T	Temperature, K or °C
T_0	Ambient temperature, K or °C
T_R	Reduced temperature, K or °C
T_{sol}	Solar temperature, K or °C
W_{net}	net electricity produced by the system, W

Abbreviations

AC	Alternating current
CHP	Combined heat and power
DH	Detached house
DHW	Domestic hot water
DM	Demand
DMC	Demand coverage percentage
LCOE	Levelized cost of energy
MTH	Mid-terraced houses
NPV	Net present value
P	Pump
PEMFC	Polymer electrolyte membrane fuel cell
PV	Photovoltaic
PV-T	Photovoltaic-thermal
SDH	Semi-detached house
SE	Stirling engine

Greek letters

β	Temperature coefficient
η	Efficiency

Subscripts/Superscripts

A	Ambient
AVG	Average
dex	Destruction
e	Electric
ELEC	Electricity
FM	Fluid
in	Input
ref	Reference
SYS	System
th	Thermal
WE	Weighted average demand met
Yr	Year

electricity, heat, or a combination of heat and electricity, and offering a host of environmental benefits [5,6]. However, PV cells face certain limitations, most notably the challenge of intermittency due to the daily solar cycle and variable weather conditions, such as cloudy skies [7]. To overcome the intermittency issue and ensure a consistent electrical supply, one promising approach involves the hybridization of solar collectors with complementary combined heat and power (CHP) technologies. A CHP system, also known as a cogeneration system, offers an efficient way to utilize energy sources by simultaneously generating electricity and heat. Efficiently hybridizing various energy technologies in CHP systems, such as diesel engines [8], fuel cells [9], or Stirling engines (SEs) [10], can play a significant role in meeting the energy demands of residential buildings in the UK.

Hybrid CHP systems often utilize multi-fuel sources (generally including one or more renewable energy sources) with high efficiency, high energy supply reliability, high energy self-sufficiency, and low greenhouse gas emissions [10–12]. These systems are typically applicable in on-grid or off-grid buildings and communities. Many hybrid CHP system-based studies that integrate diesel engines for residential applications can be found in the literature [5,13]. It is important to note that the integration of solar collectors with diesel engine generators is not suitable for single-family household use due to their noise and capacity, among other things, and these systems are more suitable for community or residential block use [14,15]. Gabrial et al. [9] studied an on-grid hybrid system in Brazil that integrated a polymer electrolyte membrane fuel cell (PEMFC), PV cells, and batteries to meet energy demands in small residential areas. However, the considerable capital cost of fuel cells at the current stage may hinder the uptake of such a hybrid technology [16,17]. SEs are particularly well-suited for small or micro-scale CHP applications [18–20]. The efficiency of a SE is theoretically close to that of the Carnot cycle, making it one of the most efficient engines available [21]. One key distinction between the SE and conventional heat engines, such as gas or diesel engines, lies in the method of heat transfer. Unlike internal combustion engines, the SE harnesses external heat transfer to drive its thermal cycle [21]. This clear separation between combustion and the thermodynamic cycle allows for individual optimization of each process. It offers several advantages, such as the ability to use different fuels (including fossil fuel, biomass, hydrogen from renewables, etc.), minimal noise levels, user-friendliness, low emissions, and high efficiency [22].

These advantages of SE well explain why many hybrid CHP-based studies that integrate SEs have been conducted by various research groups. For example, Mehregan et al. [23] investigated a hybrid CHP system that integrated a PEMFC and a β-type SE. They reported that the cogeneration system achieved a maximum efficiency of 75.5 % using optimization methods. Chen et al. [24] optimized the performance of a bio-syngas-fuelled micro-CHP system by employing Taguchi methods. The system integrated a water-cooled, unpressurized γ-type SE and a thermophotovoltaic array. The researchers reported an optimum overall efficiency of 43 %. In a study performed by Dong et al. [25], they explored a hybrid system located in Taiyuan, China, which integrated a linear Fresnel reflector subsystem, a SE, and a thermoelectric generator. The researchers investigated two distinct scenarios to evaluate the system's performance. Firstly, they examined the utilization of the

available electricity to produce hydrogen fuel through an alkaline electrolyser. Secondly, they explored the alternative approach of storing surplus electricity using a dedicated storage system. The results of their study indicate that the proposed system could generate approximately 11.73 kWh of electricity during a day, achieving an overall efficiency of 43.6 %. Açıkkalp et al. [26] conducted a study on a hybrid system that integrated a solar-driven SE, a chemical heat pump, and an absorption refrigeration system. They reported a maximum power output of 9.46 kW and an energy efficiency of 33.7 % for the system. In another study, Li et al. [27] conducted a performance analysis of a hybrid energy system. The hybrid system consisted of an alkaline fuel cell, a solar PV unit, a proton exchange membrane electrolyser, a SE, and an absorption chiller. The researchers reported an overall system efficiency of 63.8 % and reported a total exergy destruction of 73.01 kW within the system. These studies demonstrate the significant potential and increasing interest in using SE integrated systems.

On the other hand, choosing an appropriate solar-based technology to couple with SEs is not straightforward, since each solar-based technology has its pros and cons. Zhu et al. [28] investigated the feasibility of a micro-CHP system for the residential energy demand of a typical detached house in the UK. By integrating PV-T collectors, a β-type SE, and a battery-based electricity storage system, they achieved primary energy savings of 35 % and reduced carbon emissions by 37 % compared to a gas boiler and grid-based electricity reference system. Hidalgo et al. [29] studied a micro-CHP system that combines PV modules, and solar thermal collectors with a SE. The integrated system supplied 75.6 % of an average household's energy needs and achieved a significant 36.2 % reduction in CO_2 emissions. In a study performed by Incili et al. [30], they investigated a micro-CHP system integrating PV modules, a SE, and a coal boiler to heat a multi-family house in Muğla, Turkey. The SE contributed 7.7 %-14.5 % of the total thermal energy production, and the system achieved average efficiencies of 31.78 % and 30.78 % with and without the SE, respectively. For the case of the UK which has low solar irradiance and low ambient temperatures, it was demonstrated that for typical single-family household applications, a PV-T system outperforms an equivalent PV-only system in terms of both CO_2 emissions reduction potential and total energy output (electricity plus heat) [31]. This is because PV-T collectors combine PV cells and low-temperature solar thermal collectors into one integrated component and can generate both heat and electricity from the same aperture area. Therefore, integrating PV-T collectors with an SE to form a hybrid CHP system is chosen as the subject of this research.

Despite not experiencing sunlight levels comparable to sunnier regions, solar panels in the UK can still generate electricity, even on overcast days. The UK is actively investing in solar energy infrastructure, ranking as the third-largest in Europe and the tenth globally in photovoltaic (PV) capacity [32]. The UK's dedication to solar power is evident, with projections suggesting a significant increase in capacity, estimated to reach approximately 21 GW in 2025 and around 29 GW in 2030 [32]. This existing and anticipated growth underscores the technical feasibility and rationale for incorporating solar collectors in the UK.

In the UK typically detached houses (DHs), semi-detached houses (SDHs), and mid-terraced houses (MTHs) are found. The targeted house type plays an important role in determining the techno-economic feasibility of a specific CHP technology [16,33], as different house types have different floor area ranges, different energy demands and different available rooftop areas to accommodate solar panels [34]. However, in the different frameworks presented in the aforementioned studies, the influence of different house types on the techno-economic feasibility of hybrid CHP is not considered, making the potential end users for each hybrid CHP technology unclear. Furthermore, based on the literature review, it is evident that studies integrating solar-based technology with SEs are available. However, earlier studies on hybrid CHP systems were mainly based in countries at relatively low latitudes with a significant solar resource. There is a lack of research specifically focusing on the integration of solar technologies with SEs to effectively meet the actual energy demands of residential houses in the UK, which has a temperate maritime climate with lower levels of solar irradiation. A change in geography is expected to significantly affect the results, because of the different weather conditions as well as the different government policies, incentives, electricity and gas prices, household energy demands, *etc.*

Therefore, the main objective of this study is to fill these two research gaps, thus providing a deep understanding of the techno-economic and environmental performance of this type of hybrid energy system, and to estimate its applicability to the UK's different house types. To achieve this objective, a hybrid cogeneration system that combines PV-T collectors with SEs and battery-based energy options has been proposed for residential houses. The aim is to fulfil the electricity and heating requirements of different types of houses in the UK, including DHs, SDHs, and MTHs. This study includes a comprehensive assessment of the techno-economic feasibility and environmental impact assessment of the integrated energy system. Furthermore, a detailed analysis has also been conducted to determine the appropriate sizing of system components for the DH, SDH, and MTH applications.

2. Materials and methods

2.1. System topology

Fig. 1 shows the proposed topology of the integrated hybrid CHP system designed for single-family residential houses to meet the actual electricity and hot water demand. This system comprises several key components, namely a PV-T collector array, a SE-based CHP unit fuelled by natural gas, a DHW storage facility, and a battery pack for electricity storage. To facilitate the system's operation, a primary pump (Pump 1) is responsible for supplying cold water to the PV-T collector. Additionally, a secondary pump (Pump 2) is provided to feed cold water to the SE-based CHP unit. The hot water discharged from the SE unit is then mixed with hot water obtained from the outlet of the PV-T collector and stored in a DHW storage tank. Subsequently, the stored hot water at a temperature of 60 °C is readily supplied to the residential houses, to meet the space heating and DHW demand. It is important to note that the return temperature of the water from the houses is considered to be 40 °C in this system configuration.

The alternator in the SE generates alternating current (AC) electricity, and the PV-T collector array produces direct current (DC) electricity, both of which are distributed to satisfy the electrical demand load of the household via the inverter. The excess electricity will be converted into DC form and stored in the battery pack. If the state of charge of the battery reaches the high limit value and there is still surplus electricity produced by the two power supplies, this surplus electricity will be supplied to the grid. In reverse, if the electricity generated by the two power supplies cannot meet the electrical load demand of the household, the remaining load demand will be served by the battery pack. If both the two supplies and the battery pack are incapable of satisfying, electricity will be imported from the grid in this condition. For electricity storage and release, lead–carbon batteries were chosen due to their cost-effectiveness compared to lithium-ion, flow, and sodium-sulphur batteries [35]. Additionally, lead–carbon batteries outperform conventional lead-acid batteries, making them a more suitable choice for the application.

2.2. System components and modelling methodology

2.2.1. Photovoltaic-thermal collectors

Polycarbonate flat-box PV-T collectors, featuring an absorber-exchanger design with rectangular channels measuring 3 × 2 mm [36,37], have been selected in this work. These collectors offer enhanced heat transfer efficiency and cost-effectiveness when compared to the traditional copper sheet-and-tube PV-T collectors [38]. The

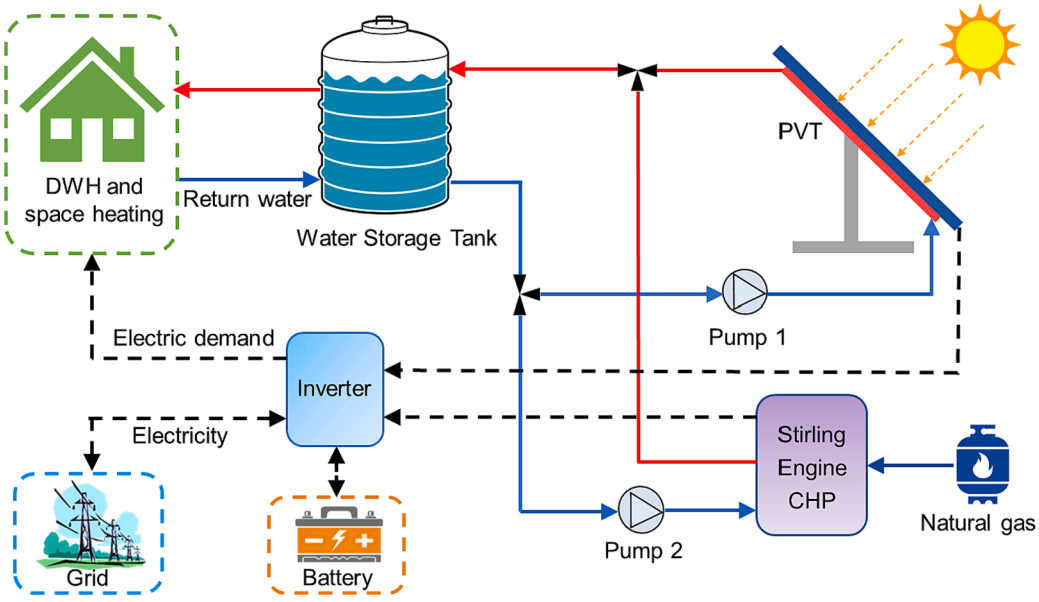

Fig. 1. System topology of PV-T-SE-battery integrated energy system.

structure of the PV-T collector consists of various components arranged in the following top-to-bottom order: a transparent glass cover, a layer of insulating gas, a multi-crystalline silicon PV module, Tedlar and Ethylene-Vinyl Acetate (EVA) layers, the absorber-exchanger, and finally, an insulation layer [36]. In the TRNSYS platform, Type 560 has been selected to model the PV-T collector. The model parameters have been adjusted to match the thermal efficiency (η_{th}) and the electrical efficiency (η_e) curves of the PV-T collectors (see Eqs. (1) and (2) below). The PV-T collector is rated at 240 W of nominal electrical power and has an aperture area of 1.55 m^2 (the considered PV-T collector numbers for DHs, SDHs, and MTHs are 18, 12, and 10, respectively). The electrical efficiency of the PV-T collector can be calculated from [31]:

$$\eta_e = \eta_{ref}\left(1+\beta\left(T_{PV}-T_{ref}\right)\right) \quad (1)$$

where η_{ref} denotes the reference PV electrical efficiency at a cell temperature of 25 °C and asolar irradiance of 1000 W/m^2, which is considered as 14.7 %, and β is the temperature coefficient (-0.45 %/K) [39]. The cell operating temperature and cell operating temperature at reference conditions have been denoted by T_{PV} and T_{ref}, respectively.

The thermal efficiency of the collector can be determined from [31]:

$$\eta_{th} = \frac{q_u}{I_{tot}} = \eta_0 - 3.325 \bullet T_R - 0.0176 \bullet I_{tot} \bullet T_R^2 \quad (2)$$

where q_u is the useful heat flow per unit area, I_{tot} is the total solar irradiance, η_0 is optical efficiency (taken as 72.6 %), and T_R is reduced temperature that can be determined from [37]:

$$T_R = \frac{T_{FM}-T_0}{I_{tot}} \quad (3)$$

where T_{FM} and T_0 are the mean temperature of the fluid and the ambient temperature respectively.

2.2.2. Stirling engine

The commercial Baxi Ecogen unit is considered in this work. It is a free-piston SE-based micro-CHP unit that is capable of generating up to 1 kW of AC electricity (with a frequency of 50 Hz) and 7.7 kW of heat simultaneously [40]. With the use of an auxiliary burner (AB), the thermal capacity of the unit can be upscaled to 24 kW.

A self-customized Type 159 model, incorporating a dynamic representation of a SE, has been successfully integrated into the TRNSYS platform. The primary objectives of this model are to accurately predict fuel consumption, as well as the production of both electricity and heat, by a SE micro-CHP unit. The sub-model adopts a grey-box modelling approach, considering the dynamic characteristics associated with four operation modes: stand-by, warming-up, full-load operation, and shutting-down. Moreover, the sub-model encompasses the SE's performance under partial load conditions. To accomplish this, the sub-model applies fundamental principles of mass and energy conservation, supported by empirical expressions derived from experimental data to determine parametric factors. The details of the SE modelling can be found in Ref. [41].

Table 1 lists the main TRNSYS types employed in the simulation of the proposed system. To well capture the shorter-term dynamics of the proposed system, dynamic simulations are performed throughout a year with a simulation time step of 2 min.

2.3. Energy analysis

The demand coverage percentage (DMC) measures the extent to which the combined electricity demand (DM_{ELEC}) and heating demand (DM_{HEAT}) of each considered household are fulfilled at a specific moment. The heating demand includes DHW and space heating of the room. The system has the potential to generate an excess or insufficient amount of electricity relative to the actual demand during that particular moment. The on-site used electricity generated from the proposed system is calculated by using the electricity demand of the household (DM_{ELEC}) subtracting the imported electricity (IM_{ELEC}). The electricity demand met (DMC_{ELEC}) and the heating demand met (DMC_{HEAT}) are calculated by [28,42]:

Table 1
Main TRNSYS types employed in the simulation of the proposed system.

Component	Type	Source
PV-T collector	Type 560	TESS component library
Stirling engine	Type 159	Self-customized
Water storage tank	Type 4	Standard library
Inverter	Type 48	Standard component library
Battery pack	Type 47	Standard component library
Pumps	Type 114	Standard component library
Differential controllers	Type 2b	Standard component library
Weather data processor	Type 15	Standard component library

$$DMC_{\mathrm{ELEC}} = \frac{DM_{\mathrm{ELEC}} - IM_{\mathrm{ELEC}}}{DM_{\mathrm{ELEC}}} \tag{4}$$

$$DMC_{\mathrm{HEAT}} = \frac{Q}{DM_{\mathrm{HEAT}}} \tag{5}$$

where Q denotes the thermal energy output of the proposed system.

To get the average measures of the combined electricity and heat demands covered by the proposed system, the average demand met (DMC_{AVG}) and the weighted average demand met (DMC_{WE}) are considered [43].

$$DMC_{\mathrm{AVG}} = \frac{DMC_{\mathrm{ELEC}} + DMC_{\mathrm{HEAT}}}{2} \tag{6}$$

$$DMC_{\mathrm{WE}} = \frac{DM_{\mathrm{ELEC}} \bullet DMC_{\mathrm{ELEC}} + DM_{\mathrm{HEAT}} \bullet DMC_{\mathrm{HEAT}}}{DM_{\mathrm{ELEC}} + DM_{\mathrm{HEAT}}} \tag{7}$$

2.4. Exergy analysis

Exergy analysis is rooted in the principles of the second law of thermodynamics, and its purpose is to assess the quality of output in relation to input within an energy conversion process. By examining the exergy destruction in various components of the integrated system, exergy analysis aids in identifying inefficiencies in the energy conversion process. This analysis provides valuable insights into the areas where exergy losses and destructions occur, highlighting opportunities for improvement and optimization. The exergy balance of the proposed cogeneration system can be written as [10]:

$$\sum Ex_{\mathrm{in}} - \sum (W_{\mathrm{net}} + Ex_{\mathrm{th}}) = \sum Ex_{\mathrm{dex}} \tag{8}$$

where Ex_{in} denotes the exergy input to the system, W_{net} is the net electricity produced by the system, Ex_{th} is the thermal exergy output of the system and Ex_{dex} is the total exergy destruction of the system. The exergy input to the system includes the exergy input from solar radiation and the fuel exergy of natural gas. The former is calculated from [10]:

$$Ex_{\mathrm{in,sol}} = A_c \bullet I_{\mathrm{tot}} \bullet \left[1 - \frac{4}{3} \bullet \frac{T_0}{T_{\mathrm{sol}}} + \frac{1}{3} \bullet \left(\frac{T_0}{T_{\mathrm{sol}}}\right)^2\right] \tag{9}$$

where A_c is the total aperture area of the PV-T collector array, T_0 is the ambient temperature in K, and T_{sol} is the solar temperature (5777 K is considered in this work [10]). The fuel exergy of natural gas is calculated with its lower heating value and chemical exergy (47 MJ/kg and 831 kJ/mol are considered [44]).

The exergy efficiency of the proposed cogeneration system, η_{Ex}, can be evaluated from:

$$\eta_{\mathrm{Ex}} = \frac{W_{\mathrm{net}} + Ex_{\mathrm{th}}}{Ex_{\mathrm{in}}} \tag{10}$$

2.5. Environmental analysis

An assessment has been conducted to determine the environmental advantages of the proposed system in terms of its potential to reduce greenhouse gas emissions. The CO_2 emission associated with the investigated system is denoted by $EM_{\mathrm{CO_2,SYS}}$, and can be calculated from can be calculated from the emission associated with the natural gas consumption plus the emission associated with the net imported electricity (imported electricity minus exported electricity) [28], i.e.,

$$EM_{\mathrm{CO_2,SYS}} = EF_{\mathrm{CO_2,gas}} \bullet NG_{\mathrm{req}} + EF_{\mathrm{CO_2,grid}} \bullet IM_{\mathrm{ELEC}} - EF_{\mathrm{CO_2,grid}} \bullet EX_{\mathrm{ELEC}} \tag{11}$$

where NG_{req} represents the amount of natural gas required to be supplied to the system from the gas network. The parameters $EF_{\mathrm{CO_2,grid}}$ and $EF_{\mathrm{CO_2,gas}}$ represent the equivalent CO_2 emission factors for grid electricity and natural gas network, respectively. For this study, the carbon emission factors for gas and electricity have been selected as 0.184 $kgCO_2$-eq/kWh [39] and 0.4116 $kgCO_2$-eq/kWh [45], respectively. EX_{ELEC} denotes the amount of exported electricity.

The total CO_2 emissions from the residential houses fitted with traditional gas boilers are denoted by $EM_{\mathrm{CO_2,ref}}$ and is defined as the sum of the emission associated with the natural gas consumption and the emission associated with the electricity consumption [46].

$$EM_{\mathrm{CO_2,ref}} = EF_{\mathrm{CO_2,gas}} \bullet NG_{\mathrm{ref}} + EF_{\mathrm{CO_2,grid}} \bullet DM_{\mathrm{ELEC}} \tag{12}$$

where NG_{ref} is the amount of natural gas consumed by the reference house.

In comparison with residential houses equipped with traditional gas boilers, the total CO_2 emissions reduction associated with the installation of the proposed system are represented by ER and can be defined as:

$$ER = EM_{\mathrm{CO_2,ref}} - EM_{\mathrm{CO_2,SYS}} \tag{13}$$

and the CO_2 emissions reduction rate, ERR, is estimated from:

$$ERR = \frac{ER}{EM_{\mathrm{CO_2,ref}}} \tag{14}$$

The total cost savings resulting from the reduction of CO_2 penalties over the lifespan of the system have been estimated using [36]:

$$CPCS = \frac{ER \bullet C_{\mathrm{CO_2}}}{d - i}\left[1 - \left(\frac{1+i}{1+d}\right)^{\mathrm{Yr}}\right] \tag{15}$$

where $C_{\mathrm{CO_2}}$ denotes the unit cost of CO_2, which exhibits a range of variability across countries, spanning from 104 £/t CO_2 to below 0.86 £/t CO_2 [36]. This variation reflects the diverse pricing mechanisms implemented by different nations. To comprehensively assess the economic and environmental viability of the suggested systems, we consider the total cost saving ($C_{\mathrm{TOT,SAV}}$) achieved through the mitigation of energy expenses and environmental penalties. The $C_{\mathrm{TOT,SAV}}$ metric quantifies the combined financial benefits derived from reduced energy bills and avoidance of penalties related to environmental impacts [47]:

$$C_{\mathrm{TOT,SAV}} = CPCS + NPV \tag{16}$$

where NPV denotes net present value and whose assessment method can be found in Section 2.6.

2.6. Economic analysis

The primary expense associated with implementing the system is primarily the initial investment, which encompasses the capital costs of various components within the integrated system. The specific capital costs for each component can be found in Table 2. Additionally, the ongoing yearly expenses consist of the component replacement, maintenance, and operational costs of the system. The lifespan of the proposed system is estimated to be 30 years, and both the inverter and the SE micro-CHP unit should be replaced after a 15-year operation, while

Table 2
Capital costs for different components of the proposed integrated energy system.

Component	Value	Unit	Source
SE micro-CHP unit (including AB)	7370	£/unit	[48]
PV-T collector array	260	£/collector	[39]
Pump station for PV-T collector	203	£/unit	[49]
Mounting	51	£/collector	[50]
Inverter	545	£/unit	[28]
Battery	227	£/kWh	[28]
Water storage tank	0.752 V_t(L) + 656.6	£	[28]
Pipes (including insulation)	9.5	£/m	[39]
System installation	34	£/m^2	[36]

the battery pack should be replaced every 10 years [28]. It is presumed that the maintenance cost of the solar system (including the PV-T collector array, water storage tank, battery pack, etc.) is 1 % of the investment cost [43], and the maintenance cost of the SE micro-CHP unit is £130 per year [34].

The net present value (*NPV*) is calculated from [42]:

$$NPV = -C_0 + \sum_{\mathrm{Yr}=1}^{t_{\mathrm{Yr}}} ACF_{\mathrm{Yr}} \frac{(1+i)^{\mathrm{Yr}-1}}{(1+d)^{\mathrm{Yr}}} \tag{17}$$

where C_0 is the total capital cost of the proposed system, the rate of inflation (2.7 % is considered in this work according to the average value of the annual inflation rate of the UK from 1989 to 2022 [51]) is denoted by i, the discount rate (3.5 % in this work [28,39]) is denoted by d and annual cash flow is denoted by ACF_{Yr}. When assessing the annual cash flow of the proposed system, the utility-price scenario of the UK in 2021 is considered, i.e., the electricity purchase price is £0.213/kWh and the natural gas price is £0.041/kWh [28]. Besides, the income due to the Smart Export Guarantee (SEG) scheme is taken into account, with a SEG tariff of £0.05/kWh [42].

The levelized cost of energy (*LCOE*) measures the lifetime cost of the system per generated energy unit and is used as an economic performance parameter for this work [36]:

$$LCOE = \frac{C_0 + \sum_{\mathrm{Yr}=1}^{t_{\mathrm{Yr}}} C_{\mathrm{O\&M\&R}} \bullet (1+i)^{\mathrm{Yr}-1} \bullet (1+d)^{-\mathrm{Yr}}}{\sum_{\mathrm{Yr}=1}^{t_{\mathrm{Yr}}} E \bullet (1+d)^{-\mathrm{Yr}}} \tag{18}$$

where $C_{\mathrm{O\&M\&R}}$ represents the annual operational (gas and electricity purchases), maintenance, and component replacement costs of the system, E denotes the net annual energy (in the form of electricity or heat) production of the proposed system. In this work, the levelized cost of electricity, $LCOE_{\mathrm{el}}$, the levelized cost of heat, $LCOE_{\mathrm{th}}$, and the levelized cost of total energy, $LCOE_{\mathrm{eq,el}}$, (consider a conversion factor of 0.48 from thermal energy to electricity [52]) were calculated.

2.7. Energy demands of different house types

In the UK, three main types of houses exist (flats are not considered in this work due to the hard constraints such as lack of roof space or building management prohibitions): DHs (shared 17.9 % of total dwellings across the UK according to the statistic in 2017 [53]), SDHs (25.0 %), and MTHs (27.4 %). To conduct the analysis presented in this work, the focus was placed on the actual energy requirements in terms of electricity and heating for these specific house types. The analysis includes a total of nine houses (all located in London, UK), with three houses representing each type: DH, SDH, and MTH. The UK Energy Research Centre Energy Data Centre has gathered and documented the hourly usage profiles of heating and electricity for these selected houses, covering an entire year [54]. These energy demand data have been chosen specifically for this analysis. Fig. 2 illustrates the annual electricity and heating demands of the chosen DH, SDH, and MTH houses. As observed in Fig. 2, the DH houses have the highest annual heating and electricity demands, followed by SDH houses, and finally MTH houses.

2.8. Optimisation

For different types of houses, the PV-T collector installation area is determined according to the guidance from the UK Energy Saving Trust [55]. In addition to the PV-T collector installation area, both the heat storage tank volume and the battery capacity play important roles in determining the techno-economic feasibility of the proposed system. An optimisation tool called GenOpt (developed by the Lawrence Berkeley National Laboratory) [56] was used to pursue the optimum values of tank volume and battery capacity that enable maximizing the NPV of the proposed system. To do so, an interface program called TRNOPT is used to couple TRNSYS with the GenOpt tool to perform the optimization. In addition, the Hooke-Jeeves algorithm (which has the advantages of fast convergence and strong adaptability) was used to find the optimum values of tank volume and battery capacity.

Fig. 3 summarizes the methodology followed in this work. Firstly, a transient model of the proposed system is developed and integrated into the TRNSYS platform for each considered house. With the weather data of London [57] and real hourly heating and electricity demand profiles of each house [54] as inputs, the key components of the proposed system are optimized for each house individually by using GenOpt. Finally, year-round simulations are conducted on each house application, and the techno-economic and environmental performance of the proposed system for different house applications are obtained accordingly.

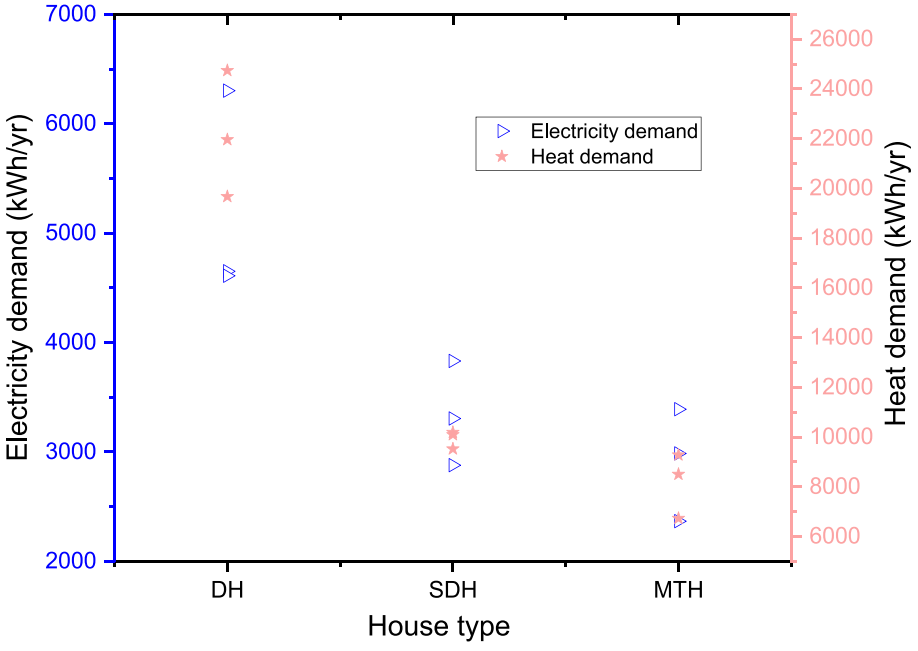

Fig. 2. Annual electricity and heating demands of DH, SDH and MTH-type houses.

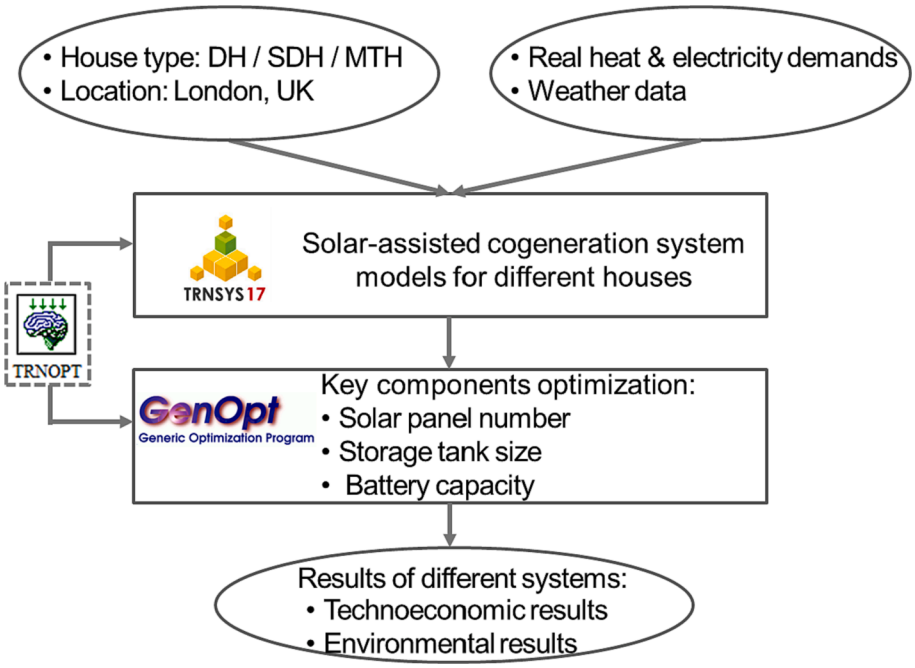

Fig. 3. Block diagram of the methodology followed in this work.

3. Results and discussion

3.1. Results of energy and exergy analysis

Table 3 presents the house profile data (including house floor area, annual electricity and demand, and annual heating demand) and the corresponding PV-T collector number, tank, and battery sizing requirements for our analysis, encompassing a total of nine houses. As previously mentioned, each house type (DH, SDH, and MTH) is represented by three houses in the analysis. The sizing requirements are based on the electricity and heating demands of the houses and obtained by using the components optimisation methodology presented in Section 2.8. According to the optimisation results of the heat storage tank volume and the battery capacity presented in Table 3, we can find that house type has a minor influence on the required tank volume. However, it has a significant influence on the required battery capacity. As the annual household electricity demand increases, the required battery capacity increases accordingly. This might be because the higher the annual household electricity demand, the greater the financial benefits that the considered system can achieve with a larger battery capacity (by avoiding electricity export and reducing electricity import).

Fig. 4(a) shows the electricity demand met (DMC_{ELEC}), heating demand met (DMC_{HEAT}), the average demand met (DMC_{AVG}), and the weighted average demand met (DMC_{WE}) for the DHs. Both DMC_{AVG} and DMC_{WE} represent the combined coverage of heating and electricity demands. The heating demand coverage (DMC_{HEAT}) for all three DHs exceeds 99 %, and this is mainly because the hybrid cogeneration systems are operated to meet the thermal demand. In terms of electricity demand coverage (DMC_{ELEC}), DH1, DH2, and DH3 are estimated to be 84.6 %, 65.2 %, and 78.9 %, respectively. DH1 has the highest DMC_{AVG}, calculated at approximately 92 %, while DH2 has the lowest at 82.2 %. Similarly, DH1 has the highest DMC_{WE}, calculated at approximately 96.9 %, while DH2 has the lowest at 92.3 %.

Fig. 4(b) shows the electricity demand met (DMC_{ELEC}), heating demand met (DMC_{HEAT}), the average demand met (DMC_{AVG}), and the weighted average demand met (DMC_{WE}) for the SDHs. The trend observed for DMC_{HEAT} in the SDHs is similar to that observed in the DHs, with all three houses exceeding 99 % coverage. In terms of electricity demand coverage (DMC_{ELEC}), SDH1, SDH2, and SDH3 are estimated to be 69.5 %, 62.5 %, and 74.8 %, respectively. Among the SDHs, SDH3 has the highest DMC_{AVG}, calculated at approximately 87.3 %, while SDH2 has the lowest at 81.2 %. Similarly, SDH3 has the highest DMC_{WE}, calculated at approximately 94.3 %, while SDH2 has the lowest at 89.6 %.

Fig. 4(c) shows the electricity demand met (DMC_{ELEC}), heating demand met (DMC_{HEAT}), the average demand met (DMC_{AVG}), and the weighted average demand met (DMC_{WE}) for the MTHs. The heating demand coverage (DMC_{HEAT}) for all three MTHs achieved 100 %. In terms of electricity demand coverage (DMC_{ELEC}), MTH1, MTH2, and MTH3 are estimated to be 57.7 %, 57.4 %, and 79.6 %, respectively.

Table 3
House profile data and corresponding PV, tank and battery sizing requirements.

House number	Floor area (m^2)	Electricity demand (kWh/yr)	Heating demand (kWh/yr)	PV-T collector number	Optimized tank volume (L)	Optimized battery capacity (kWh)
DH1	136.1	4650	21,953	18	650	4.13
DH2	183.9	6302	24,739	18	143	3.66
DH3	128	4609	19,668	18	812	4.61
SDH1	74.3	3305	9514	12	487	2.62
SDH2	74.3	3831	10,087	12	587	2.07
SDH3	74.3	2878	10,179	12	825	2.86
MTH1	68.8	2985	6726	10	437	2.23
MTH2	60.3	3390	8497	10	650	2.07
MTH3	68.8	2366	9272	10	562	2.15

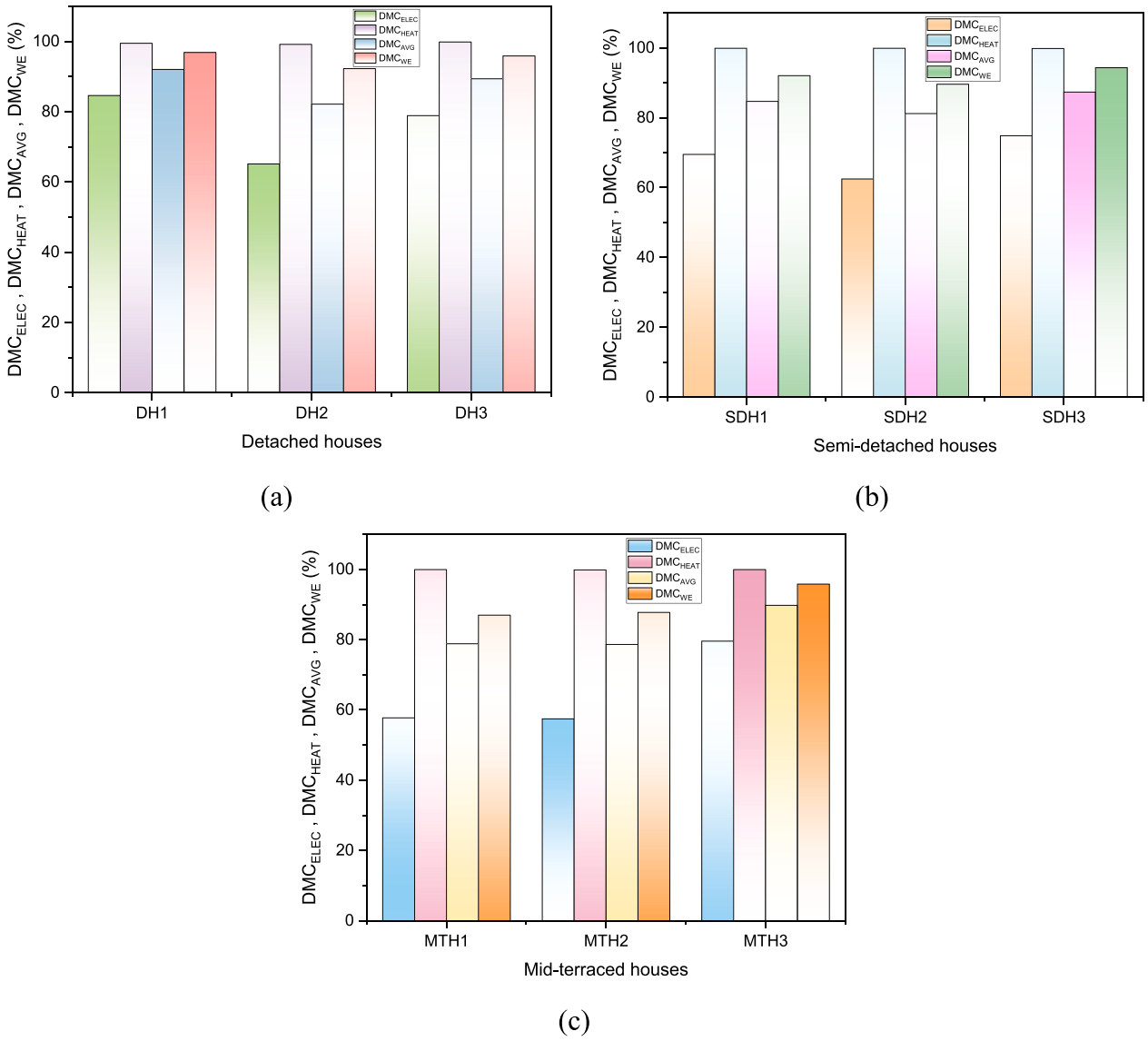

Fig. 4. DMC_{ELEC}, DMC_{HEAT}, DMC_{AVG}, and DMC_{WE} of the system for (a) DH, (b) SDH, and (c) MTH configurations.

Among the MTHs, MTH3 has the highest DMC_{AVG}, calculated at approximately 89.8 %, while MTH2 has the lowest at 78.6 %. Similarly, MTH3 has the highest DMC_{WE}, calculated at approximately 95.8 %, while MTH1 has the lowest at 87 %.

The results of the exergy analysis for the proposed integrated energy system in three distinct housing types, namely DHs, SDHs, and MTHs, are presented in Fig. 5. This analysis offers valuable insights into the efficiency of the integrated system throughout the year, from January to December. In Fig. 5(a), the exergy efficiency of the integrated system for DHs is illustrated, with DH1 displaying the highest efficiency of 22 % found in December. This indicates that the integrated system for DH1 effectively utilizes and converts available energy resources into useful work. The exergy efficiency in January is at a higher level, it starts to decrease in the further months and reaches a bottom in July, then further it starts to increase and reach a peak in December. It is important to note that the efficiency of the SE-based CHP system is higher compared to solar-based technologies. During the summer months, the PV-T system operates more frequently than the SEs. As a result, the integrated exergy efficiency of the system tends to be lower during this time. However, in the winter months, SEs operate for longer periods. Consequently, the integrated exergy efficiency of the system is found to be higher during the winter period. On the other hand, the system for the DH2 house exhibits the lowest exergy efficiency at 11 % in August, indicating a lower level of energy utilization and conversion efficiency compared to other DHs.

Moving on to Fig. 5(b), which represents the exergy efficiency of the integrated system for SDHs, the integrated system for the SDH2 house emerges as the most efficient, with a maximum exergy efficiency of 20 % in December. SDH2 effectively harnesses energy resources and converts them into useful work. Conversely, the integrated system for SDH1 demonstrates the lowest exergy efficiency among the three SDHs, with a value of 12 % in July. This suggests a relatively lower level of energy utilization and conversion efficiency in SDH1 compared to its counterparts.

Fig. 5(c) showcases the exergy efficiency of the integrated system for MTHs. Among the three MTHs, MTH3 stands out with the highest exergy efficiency at 20 % in December. The integrated system for MTH3 effectively optimizes energy utilization and conversion. Conversely, the integrated system for MTH1 exhibits the lowest exergy efficiency at 12 % in July, indicating a comparatively lower level of energy utilization and conversion efficiency within that particular MTH.

These findings provide crucial information about the performance and efficiency of the integrated energy system in different types of houses. By identifying the integrated systems for houses with the highest

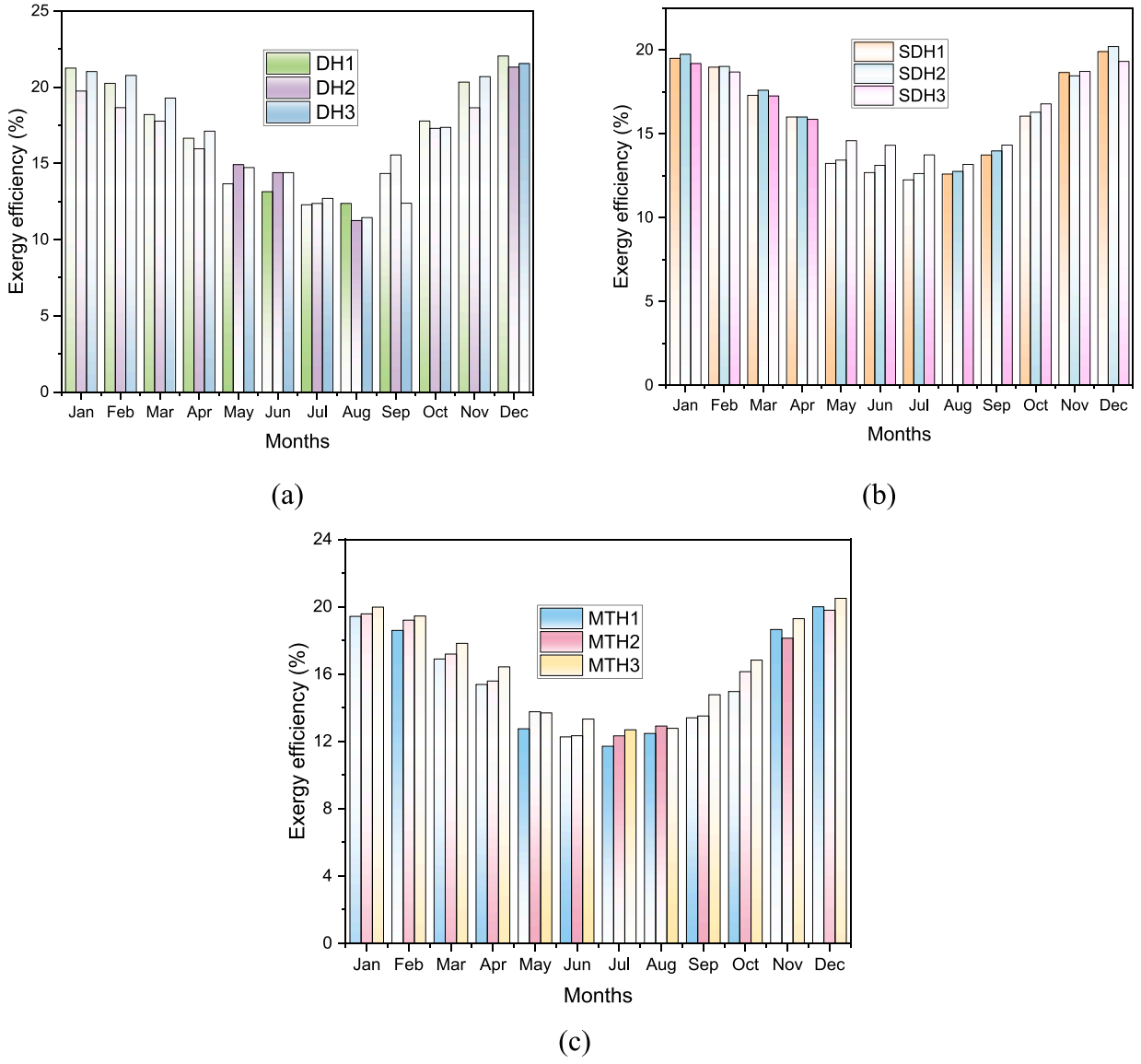

Fig. 5. Exergy efficiency of the system for (a) DH, (b) SDH, and (c) MTH configurations.

and lowest exergy efficiencies, it becomes possible to focus on optimizing energy utilization and conversion processes, thereby enhancing overall energy efficiency and sustainability in residential buildings.

3.2. Results of environmental analysis

Fig. 6(a) illustrates the overall reduction in CO_2 emissions achieved by residential DHs equipped with traditional gas boilers. According to estimates, the potential reductions in CO_2 emissions for DH1, DH2, and DH3 houses are 2447 kg CO_2-eq, 2448 kg CO_2-eq, and 2348 kg CO_2-eq, respectively. The corresponding CO_2 emissions reduction rates are 37 %, 31 % and 38 %, respectively. Similarly, Fig. 6(b) showcases the total CO_2 emissions reduction associated with residential SDHs that have traditional gas boilers. It is estimated that SDH1, SDH2, and SDH3 houses could achieve reductions of 1328 kg CO_2-eq, 1372 kg CO_2-eq, and 1446 kg CO_2-eq, respectively (CO_2 emissions reduction rates are 39 %, 36 % and 43 %, respectively). Likewise, Fig. 6(c) shows the CO_2 emissions reduction potential for residential MTHs equipped with traditional gas boilers. The estimated reductions for MTH1, MTH2, and MTH3 houses are 1063 kg CO_2-eq, 1124 kg CO_2-eq, and 1187 kg CO_2-eq, respectively (CO_2 emissions reduction rates are 40 %, 35 % and 40 %, respectively).

The results presented In Fig. 6 demonstrate a clear trend, indicating that DH configurations achieve the highest overall reduction in CO_2 emissions compared to SDH and MTH configurations. One of the primary reasons behind this performance disparity lies in the differences in the PV-T system sizes employed in each configuration. As observed, DH configurations utilize larger PV-T systems, followed by SDH and MTH configurations. Upon closer examination of Table 3, it becomes evident that DH houses are equipped with 18 PV-T collectors, whereas SDH configurations have 12 collectors, and MTH configurations have 10 collectors. This difference in the number of PV-T collectors directly influences the energy generation capacity of each system. The larger PV-T system in DH configurations allows for greater production of both electricity and thermal energy, leading to a more significant reduction amount in overall CO_2 emissions. The higher number of PV-T collectors and the corresponding increased energy generation capacity of DH configurations contribute to their superior performance in reducing CO_2 emissions. As a result, DH configurations achieve the highest overall reduction in CO_2 emissions compared to SDH and MTH configurations. However, in terms of the achieved CO_2 emissions reduction rates, there is no big difference in different house types, all within the range of 30 % to 45 %. This implies the carbon emission reduction rate of the proposed

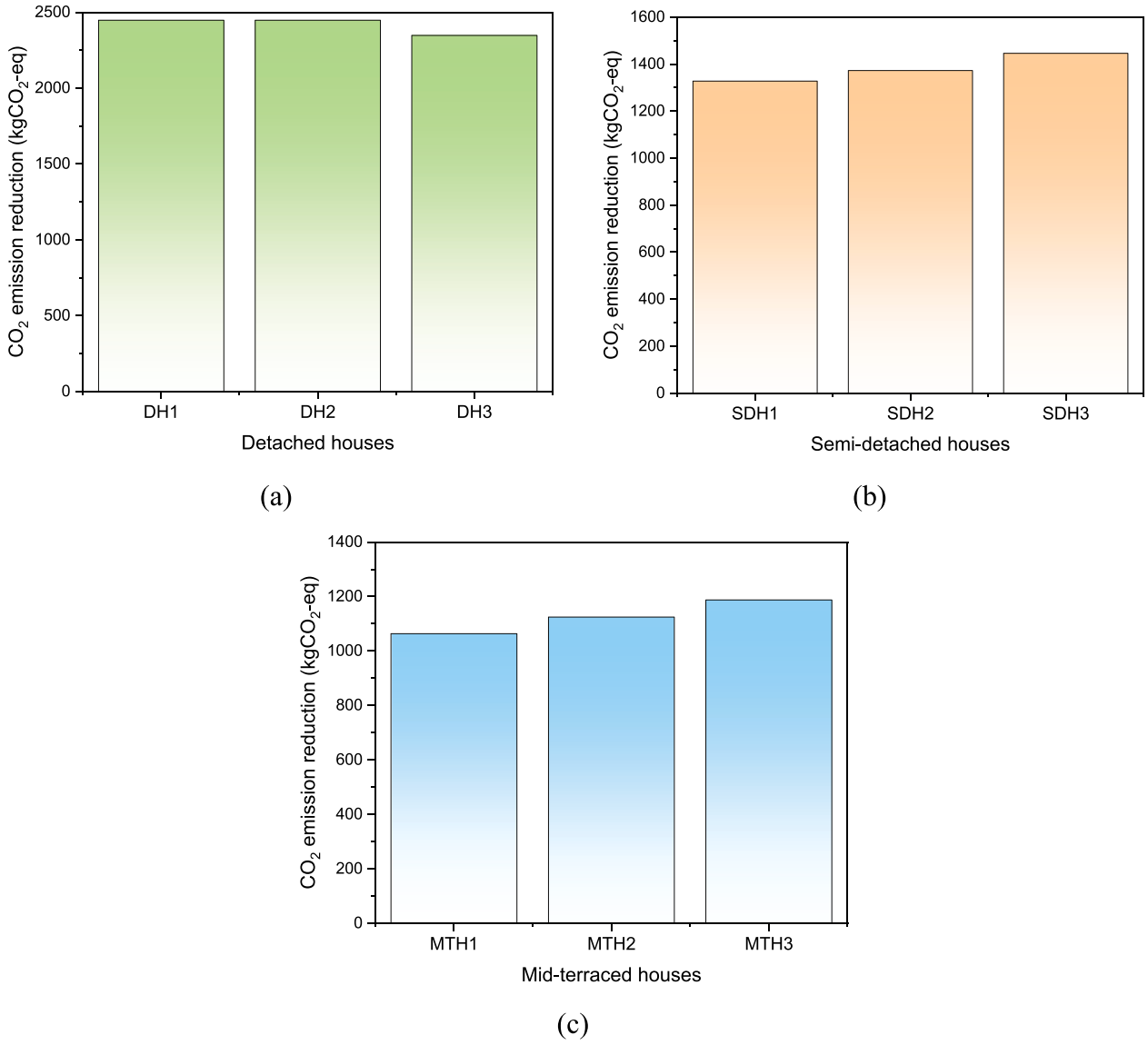

Fig. 6. CO_2 emission reduction of the system for (a) DH, (b) SDH, and (c) MTH configurations.

hybrid cogeneration system is not sensitive to the house type, up to a point.

It is important to note that the implementation or scheduled implementation of carbon tax and emission trading systems may lead to additional costs for energy usage due to CO_2 emissions. The carbon prices vary across different countries, ranging from £0.86/t CO_2 to £104/t CO_2 [36]. These variations in carbon prices are used to estimate the potential range of CPCS, as indicated by the bottom and top error bars. The sensitivity of CPCS for DH, SDH, and MTH configurations is illustrated in Fig. 7. Fig. 7(a) demonstrates that for DH configurations, when the carbon price is set to the high limit (£104/t CO_2), the CPCS exceeds £6500. In Fig. 7(b), it is shown that for SDH configurations, with a carbon price set to the high limit, the CPCS goes beyond £3500. Fig. 7 (c) reveals that for MTH2 and MTH3 houses if the carbon price is set to the high limit, the CPCS rises above £3000. However, for MTH1, the CPCS remains below £3000.

A sensitivity analysis is conducted to examine the impact of mitigating energy expenses and environmental penalties on the total cost savings ($C_{TOT,SAV}$).The range of carbon prices is used to estimate the potential variations in $C_{TOT,SAV}$. The sensitivity of $C_{TOT,SAV}$ for DH, SDH, and MTH houses is shown in Fig. 8. Fig. 8(a) illustrates that for DH2 configuration, when the carbon price is set to the high limit (£104/t CO_2), the $C_{TOT,SAV}$ reaches £9000. However, for DH3, the $C_{TOT,SAV}$ reaches £6000. In Fig. 8(b), it is observed that for all SDH configurations, when the carbon price is set to the high limit, $C_{TOT,SAV}$ remains in negative territory. Similarly, Fig. 8(c) demonstrates that the trends for MTH houses are also consistent, where the $C_{TOT,SAV}$ remains negative when the carbon price is set to the high limit.

This implies the applicability of the proposed system to DH is best among the three analysed house types, and such a system is not an unattractive solution for SDHs and MTHs from a perspective that combines economic and environmental. However, it should be noted this conclusion is drawn based on the utility-price scenario in 2021 and fixed inflation and discount rates. As found in our previous research, both utility prices and inflation and discount rates have a great influence on the economic performance of a solar-based system [38,43]. For example, for a similar system but for a specific DH application, the NPV of the system will increase from £1990 to £19,400 (increased by 8.5 times) if the utility price changes from the scenario of 2021 to the scenario of early 2023, and the payback period decreases from 28 years to 11 years [28]. Therefore, it is anticipated that with utility prices increase (which is occurring given recent trends), better economic performance can be achieved for the application of the proposed system to SDHs and MTHs, and the applicability of the proposed system to the two types of houses

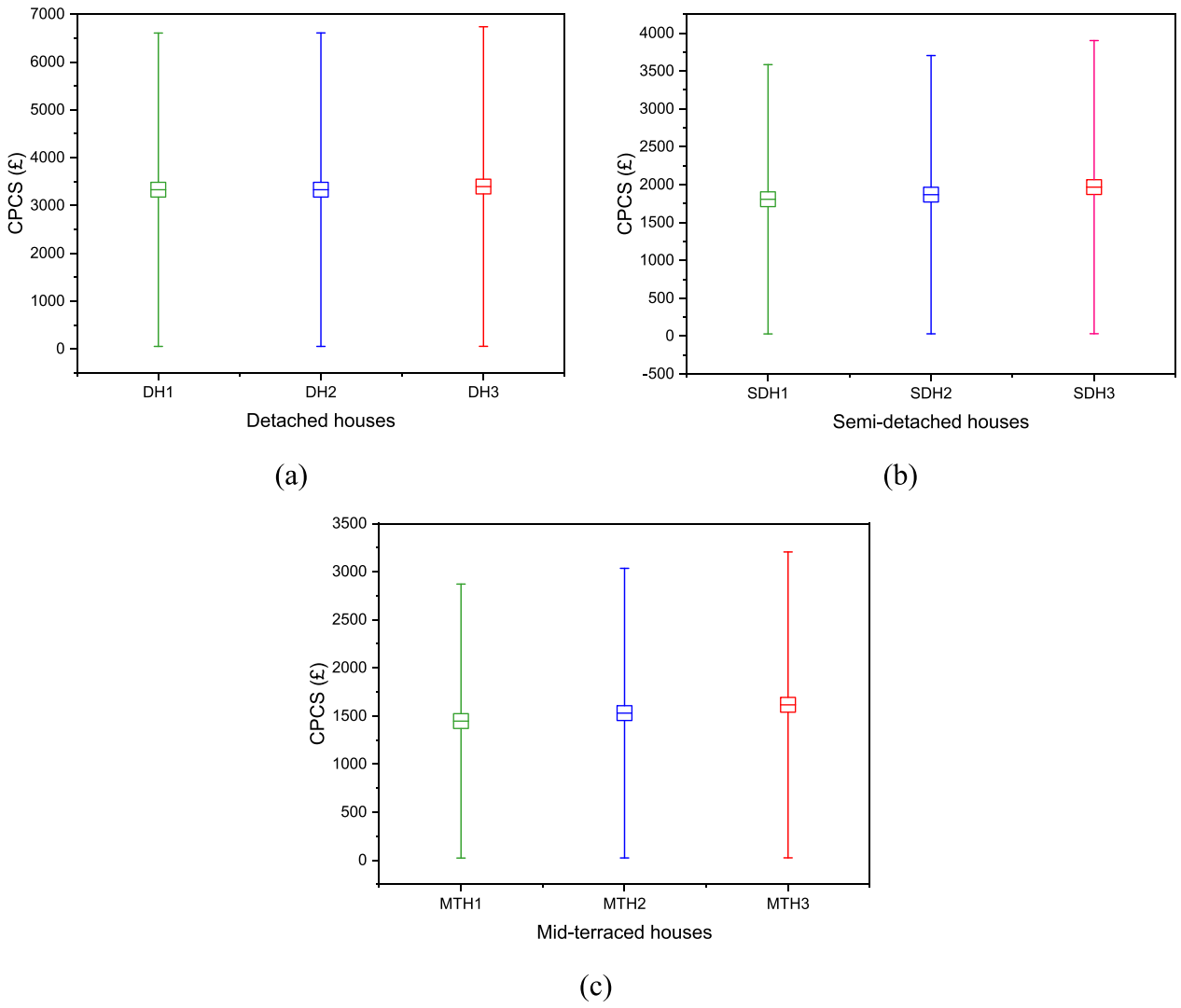

Fig. 7. Sensitivity of CPCS for (a) DH, (b) SDH, and (c) MTH configurations.

will become better.

3.3. Results of economic analysis

The economic analysis results of the integrated energy systems in three distinct housing types – DHs, SDHs, and MTHs – are presented in this section. The *LCOE* values for electricity ($LCOE_{el}$), thermal energy ($LCOE_{th}$) and the combined equivalent electricity ($LCOE_{eq,el}$) are displayed in Fig. 9(a) for all three DH houses. Upon analysing the results, it is observed that the DH configurations display variations in their *LCOE* values. DH1 has the lowest $LCOE_{el}$ value at 0.622 £/kWh, making it the most cost-effective option for electricity. On the other hand, DH2 shows the highest $LCOE_{el}$ value at 0.761 £/kWh, suggesting that it is relatively less economically favourable for electricity generation within the DH group. Regarding thermal energy costs, DH1 also stands out with the minimum $LCOE_{th}$ value of 0.147 £/kWh, indicating its superior cost efficiency for heat production. Conversely, DH3 exhibits the maximum $LCOE_{th}$ value at 0.161 £/kWh, making it less economical for thermal energy generation within the DH category. Lastly, when considering the overall cost efficiency of electricity generation $LCOE_{eq,el}$, DH2 shows the highest value at 0.23 £/kWh, while DH1 demonstrates the lowest at 0.205 £/kWh, solidifying DH1 as the most economically viable option in this respect.

Moving on to Fig. 9(b), which presents the *LCOE* values for the three SDH houses, similar variations can be observed. SDH3 emerges with the minimum $LCOE_{el}$ value at 0.799 £/kWh, indicating its cost advantage for electricity generation. On the other hand, SDH2 exhibits the maximum $LCOE_{el}$ value at 0.862 £/kWh, suggesting it is comparatively less economically favourable in terms of electricity costs within the SDH group. Regarding thermal energy expenses, SDH3 demonstrates the lowest $LCOE_{th}$ value at 0.224 £/kWh, making it the most cost-efficient option for heat generation. Conversely, SDH2 exhibits the highest $LCOE_{th}$ value at 0.247 £/kWh, implying it is the least economically advantageous for thermal energy production among the SDH configurations. Furthermore, when considering the overall cost efficiency of electricity generation $LCOE_{eq,el}$, SDH2 has the highest value at 0.322 £/kWh, while SDH3 boasts the lowest value at 0.294 £/kWh, solidifying SDH3 as the most economically viable option in this aspect.

Additionally, Fig. 9(c) presents the *LCOE* values for the three MTH houses. Among them, MTH3 exhibits the minimum $LCOE_{el}$ value at 0.82 £/kWh, indicating its cost advantage for electricity generation within the MTH group. Conversely, MTH2 demonstrates the maximum $LCOE_{el}$ value at 0.978 £/kWh, suggesting it is less economically favourable for electricity generation compared to other MTH configurations. Regarding thermal energy costs, MTH3 also stands out with the lowest $LCOE_{th}$ value at 0.226 £/kWh, signifying its superior cost efficiency for heat production. On the other hand, MTH1 exhibits the maximum $LCOE_{th}$ value at 0.322 £/kWh, making it the least economically

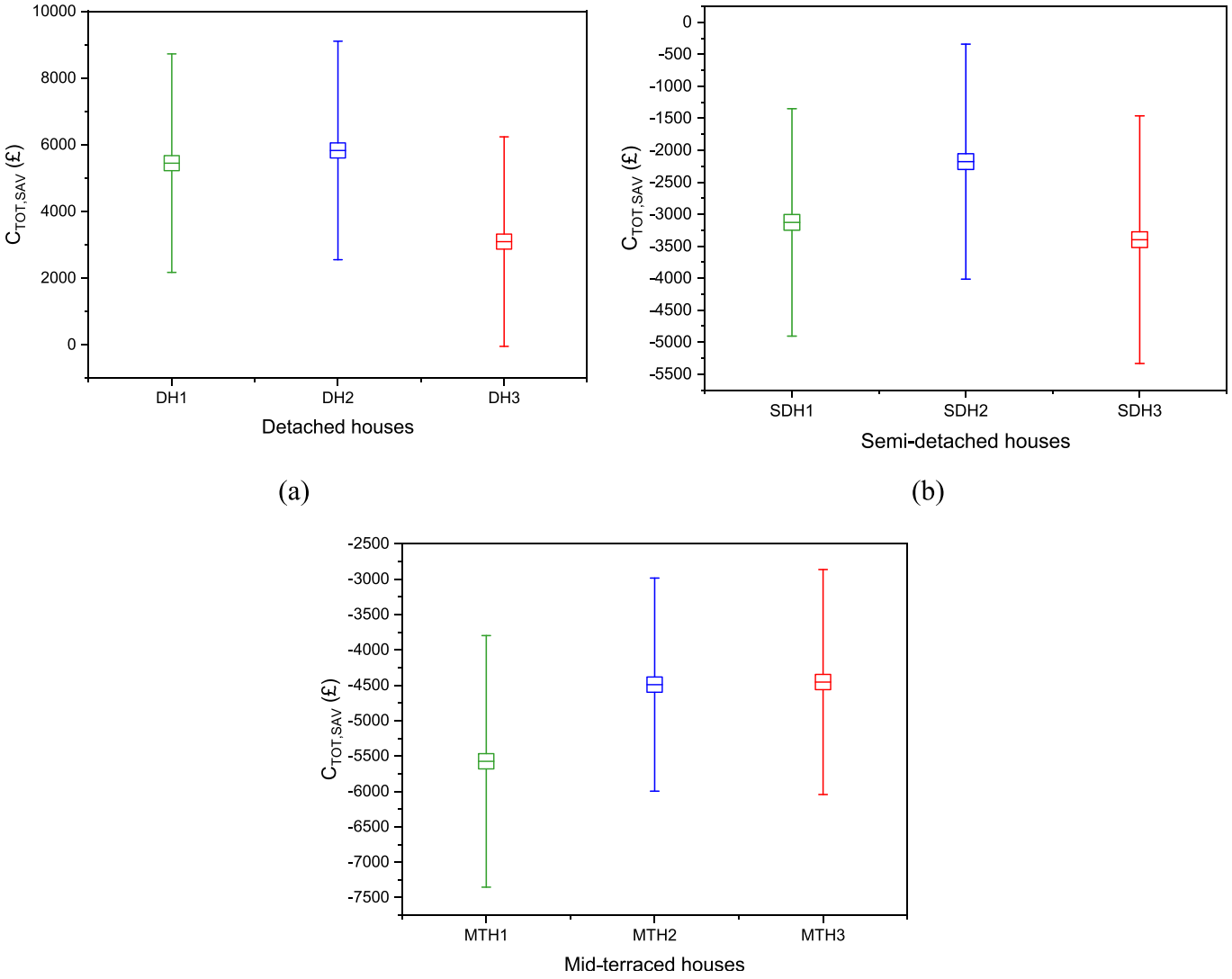

Fig. 8. Sensitivity of $C_{TOT,SAV}$ for (a) DH, (b) SDH, and (c) MTH configurations.

advantageous for thermal energy generation within the MTH category. Moreover, when considering the overall cost efficiency of electricity generation $LCOE_{eq,el}$, MTH1 displays the highest value at 0.398 £/kWh, while MTH3 demonstrates the lowest value at 0.299 £/kWh, reaffirming MTH3 as the most economically viable option in this regard.

The observed variations in *LCOE* values can be attributed to the differences in integrated system exergy efficiency among the housing types. DH configurations exhibit higher exergy efficiency compared to SDH and MTH configurations, as illustrated in Fig. 5. This higher exergy efficiency in DHs leads to reduced operational costs and ultimately results in the comparatively lower *LCOE* values observed in this study. Thus, resulting in the superior economic performance of DHs, followed by SDHs and MTHs. The findings highlight the importance of considering the specific housing type and its integrated energy system efficiency when assessing the economic viability of such systems for sustainable energy production and utilization.

4. Conclusions and further discussion

In this research, a novel hybrid cogeneration system designed to address the electricity and heating needs of residential houses in the UK is presented. The system combines photovoltaic-thermal collectors, Stirling engines, and battery-based energy options. The study encompasses an in-depth evaluation of the techno-economic feasibility and environmental impact of this integrated energy system for three types of houses: detached houses (DHs), semi-detached houses (SDHs), and mid-terraced houses (MTHs).

Key findings from our investigation are summarized below:

- The integrated system for DHs (with a 1 kWe-Stirling engine plus 28 m^2 of photovoltaic-thermal collector array) exhibits higher exergy efficiency compared to the configurations for SDHs and MTHs, with the peak efficiency reaching 22 %.
- Among the three types of houses, DHs stand out as the most economically viable option. They boast the lowest levelized cost of electricity (*LCOE*) at 0.622 £/kWh, the lowest levelized cost of heat ($LCOE_{th}$) at 0.147 £/kWh, and the lowest levelized cost of total energy ($LCOE_{eq,el}$) at 0.205 £/kWh.
- DHs demonstrate the highest potential for reducing carbon dioxide (CO_2) emissions amount. However, the carbon emission reduction rate of the proposed hybrid cogeneration system is not sensitive to the house type, up to a point. All of the achieved carbon emission reduction rates are within the range of 30 % to 45 %.
- When evaluating the applicability of the system to the three house types, it is evident that the system is most suitable for DHs, followed by SDHs and MTHs, in descending order.

This study introduces an innovative hybrid cogeneration system

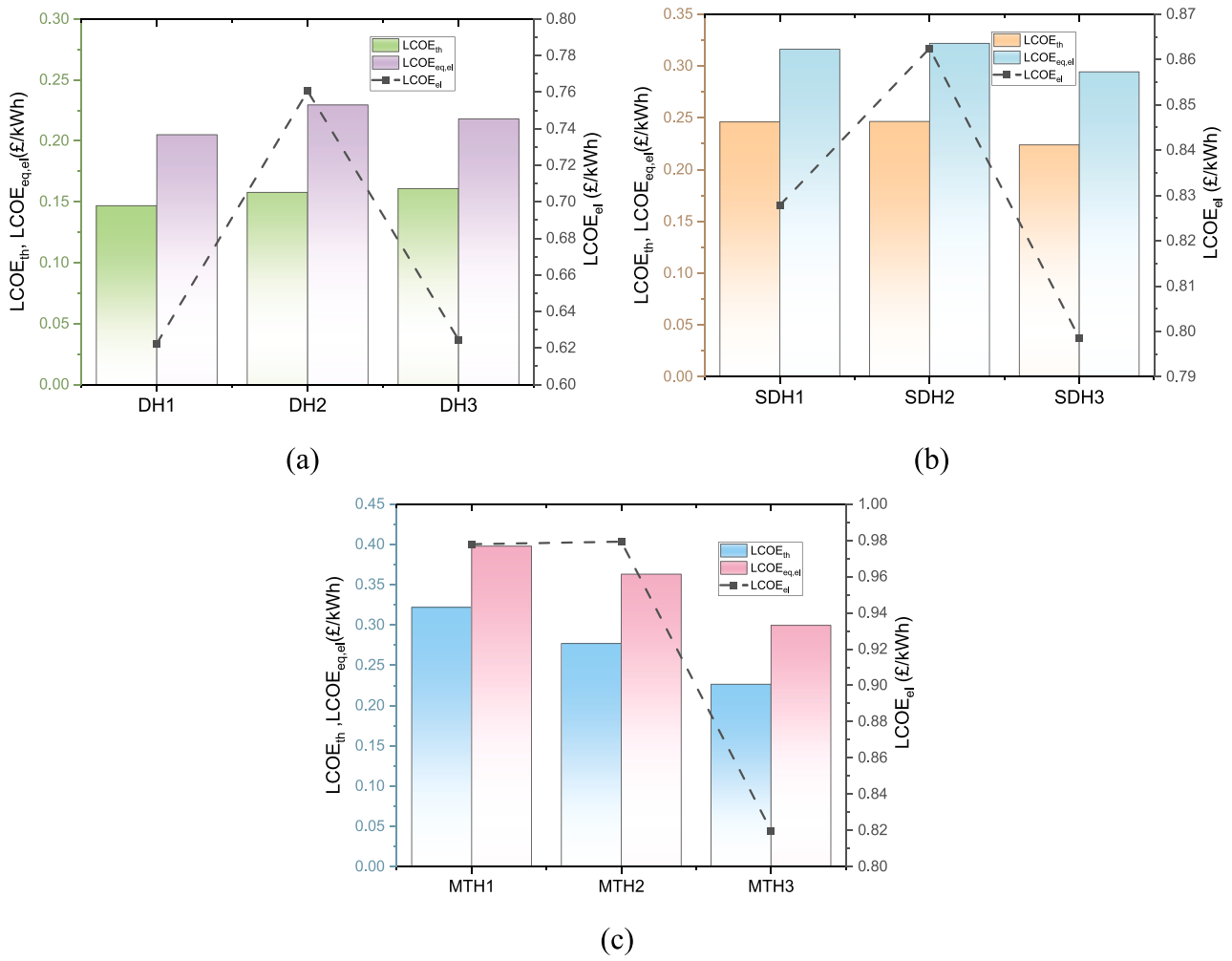

Fig. 9. $LCOE_{th}$, $LOCE_{el}$ and $LCOE_{eq,el}$ of the system for (a) DH, (b) SDH, and (c) MTH configurations.

capable of fulfilling the electrical and heating demands of various residential houses in the UK. The system's superior exergy efficiency, economic viability, and substantial emission reduction potential make it a promising candidate for sustainable energy solutions. Our analyses indicate that DHs are identified as the most suitable application for this integrated energy system, with notable advantages over other housing types. Such assessment can inform system developers who are the potential consumers of the considered system. Besides, it also helps policymakers to critique existing and potential new policies and regulations surrounding the promotion of hybrid cogeneration systems.

It is important to note that the proposed hybrid cogeneration system has a significant potential to lower carbon emissions and the primary energy consumed by households. Such a system integrates two main technologies, i.e., Stirling engine micro-CHP and photovoltaic-thermal collectors, both of which are already commercially available. It has been shown that the integrated systems can be optimised for particular installations, in particular by optimizing the energy storage components. One of the major challenges of integrating PV-T collectors and Stirling engines is the high upfront investment cost of such a system, especially arising from the Stirling engines and the photovoltaic-thermal collectors, which act as a barrier to widespread penetration at present.

It is anticipated that with the initial investment reduced, the proposed solar-based CHP system could emerge as an important solution in achieving the net-zero goal by 2050 in the UK. The energy models and methodology presented in the analysis are straightforward and can be applied to other countries for building similar CHP systems based on the specific energy demands of houses in those countries. In terms of future research, it will be an interesting prospect to investigate other configurations for example setting a common system designed to provide energy to two SDH houses.

CRediT authorship contribution statement

Dibyendu Roy: Conceptualization, Formal analysis, Investigation, Methodology, Visualization, Writing – original draft. **Shunmin Zhu:** Conceptualization, Funding acquisition, Software, Supervision, Writing – review & editing. **Ruiqi Wang:** Validation, Visualization. **Iker González-Pino:** Software, Writing – review & editing. **María Herrando:** Software, Writing – review & editing. **Christos N. Markides:** Funding acquisition, Writing – review & editing. **Anthony Paul Roskilly:** Resources, Funding acquisition.

Declaration of competing interest

The authors declare that they have no known competing financial interests or personal relationships that could have appeared to influence the work reported in this paper.

Data availability

Data will be made available on request.

Acknowledgments

This work was supported by the UK Engineering and Physical Sciences Research Council (EPSRC) [grant numbers EP/T022949/1, EP/M025012/1, and EP/R045518/1], and by the Royal Society via an International Collaboration Award 2020 [grant number ICA\R1\201302]. The authors would like to thank UK company Solar Flow Ltd. (www.solar-flow.co.uk). Data supporting this publication can be obtained on request from cep-lab@imperial.ac.uk. For the purpose of Open Access, the authors have applied a CC BY public copyright licence to any Author Accepted Manuscript version arising from this submission.

References

[1] Climate Change Committee. Independent Assessment: The UK's Heat and Buildings Strategy; 2022.
[2] Government HM. Heat Build Strategy 2021.
[3] BEIS. Net Zero Strategy: Build Back Greener; 2021.
[4] Zhou K, Zhu S, Wang Y, Roskilly AP. Modelling and experimental characterization of a water-to-air thermoelectric heat pump with thermal energy storage. Energies 2024;17(2):414. https://doi.org/10.3390/en17020414.
[5] Nosrat AH, Swan LG, Pearce JM. Simulations of greenhouse gas emission reductions from low-cost hybrid solar photovoltaic and cogeneration systems for new communities. Sustain Energy Technol Assessments 2014;8:34–41. https://doi.org/10.1016/j.seta.2014.06.008.
[6] Herrando M, Wang K, Huang G, Otanicar T, Mousa OB, Agathokleous RA, et al. A review of solar hybrid photovoltaic-thermal (PV-T) collectors and systems. Prog Energy Combust Sci 2023;97:101072. https://doi.org/10.1016/J.PECS.2023.101072.
[7] Pearce JM. Expanding photovoltaic penetration with residential distributed generation from hybrid solar photovoltaic and combined heat and power systems. Energy 2009;34:1947–54. https://doi.org/10.1016/j.energy.2009.08.012.
[8] Rangel N, Li H, Aristidou P. An optimisation tool for minimising fuel consumption, costs and emissions from Diesel-PV-Battery hybrid microgrids. Appl Energy 2023;335. https://doi.org/10.1016/j.apenergy.2023.120748.
[9] de Oliveira Gabriel R, de Souza Laya Junior E, Leal Braga S, Pradelle F, Torres Serra E, Coutinho Sobral Vieira CL. Technical, economic and environmental analysis of a hybrid CHP system with a 5 kW PEMFC, photovoltaic panels and batteries in the Brazilian scenario. Energy Convers Manag 2022;269:116042. https://doi.org/10.1016/j.enconman.2022.116042.
[10] Kallio S, Siroux M. Exergy and exergo-economic analysis of a hybrid renewable energy system under different climate conditions. Renew Energy 2022;194:396–414. https://doi.org/10.1016/j.renene.2022.05.115.
[11] Martinez S, Michaux G, Salagnac P, Bouvier JL. Micro-combined heat and power systems (micro-CHP) based on renewable energy sources. Energy Convers Manag 2017;154:262–85. https://doi.org/10.1016/j.enconman.2017.10.035.
[12] Kallio S, Siroux M. Hybrid renewable energy systems based on micro-cogeneration. Energy Rep 2022;8:762–9. https://doi.org/10.1016/j.egyr.2021.11.158.
[13] Lissén JMS, Rodríguez LR, Parejo FD, de la Flor FJS. An economic, energy, and environmental analysis of PV/Micro-CHP hybrid systems: a case study of a tertiary building. Sustain 2018;10:1–15. https://doi.org/10.3390/su10114082.
[14] Phuangpornpitak N, Kumar S. User acceptance of diesel/PV hybrid system in an island community. Renew Energy 2011;36:125–31. https://doi.org/10.1016/j.renene.2010.06.007.
[15] Romero Rodríguez L, Salmerón Lissén JM, Sánchez Ramos J, Rodríguez Jara EÁ, Álvarez DS. Analysis of the economic feasibility and reduction of a building's energy consumption and emissions when integrating hybrid solar thermal/PV/micro-CHP systems. Appl Energy 2016;165:828–38. https://doi.org/10.1016/j.apenergy.2015.12.080.
[16] Hammond GP, Titley AA. Small-scale combined heat and power systems: the prospects for a distributed micro-generator in the 'net-zero' transition within the UK. Energies 2022;15. https://doi.org/10.3390/en15166049.
[17] Elmer T, Worall M, Wu S, Riffat SB. Fuel cell technology for domestic built environment applications: state of-the-art review. Renew Sustain Energy Rev 2015;42:913–31. https://doi.org/10.1016/j.rser.2014.10.080.
[18] Zhu S, Yu G, Liang K, Dai W, Luo E. A review of Stirling-engine-based combined heat and power technology. Appl Energy 2021;294:116965. https://doi.org/10.1016/j.apenergy.2021.116965.
[19] Zhu S, Yu G, O J, Xu T, Wu Z, Dai W, et al. Modeling and experimental investigation of a free-piston Stirling engine-based micro-combined heat and power system. Appl Energy 2018;226:522–33. https://doi.org/10.1016/j.apenergy.2018.05.122.
[20] Jiang Z, Yu G, Zhu S, Dai W, Luo E. Advances on a free-piston Stirling engine-based micro-combined heat and power system. Appl Therm Eng 2022;217:119187. https://doi.org/10.1016/J.APPLTHERMALENG.2022.119187.
[21] Schneider T, Müller D, Karl J. A review of thermochemical biomass conversion combined with Stirling engines for the small-scale cogeneration of heat and power. Renew Sustain Energy Rev 2020;134:110288. https://doi.org/10.1016/j.rser.2020.110288.
[22] Chen Y, Yu G, Ma Y, Xue J, Ahmed F, Cheng Y, et al. A thermally-coupled cascade free-piston Stirling engine-based cogeneration system. Appl Therm Eng 2024;236:121679. https://doi.org/10.1016/J.APPLTHERMALENG.2023.121679.
[23] Mehregan M, Sheykhi M, Alizadeh Kharkeshi B, Emamian A, Aliakbari K, Rafiee N. Performance analysis and optimization of combined heat and power system based on PEM fuel cell and β type Stirling engine. Energy Convers Manag 2023;283:116874. https://doi.org/10.1016/j.enconman.2023.116874.
[24] Chen WL, Currao G, Li YH, Kao CC. Employing Taguchi method to optimize the performance of a microscale combined heat and power system with Stirling engine and thermophotovoltaic array. Energy 2023;270:126897. https://doi.org/10.1016/j.energy.2023.126897.
[25] Dong H, Guo Je, Liu J, Meng T, Li M, Chen X, et al. Energy generation and storing electrical energy in an energy hybrid system consisting of solar thermal collector, Stirling engine and thermoelectric generator. Sustain Cities Soc 2021;75. https://doi.org/10.1016/j.scs.2021.103357.
[26] Açıkkalp E, Kandemir SY, Ahmadi MH. Solar driven Stirling engine – chemical heat pump – absorption refrigerator hybrid system as environmental friendly energy system. J Environ Manage 2019;232:455–61. https://doi.org/10.1016/j.jenvman.2018.11.055.
[27] Li D, Guo J, Zhang J, Zhan L, Alizadeh M. Numerical assessment of a hybrid energy generation process and energy storage system based on alkaline fuel cell, solar energy and Stirling engine. J Energy Storage 2021;39:102631. https://doi.org/10.1016/j.est.2021.102631.
[28] Zhu S, Wang K, González-Pino I, Song J, Yu G, Luo E, et al. Techno-economic analysis of a combined heat and power system integrating hybrid photovoltaic-thermal collectors, a Stirling engine and energy storage. Energy Convers Manag 2023;284. https://doi.org/10.1016/j.enconman.2023.116968.
[29] Auñón-Hidalgo JA, Sidrach-de-Cardona M, Auñón-Rodríguez F. Performance and CO2 emissions assessment of a novel combined solar photovoltaic and thermal, with a Stirling engine micro-CHP system for domestic environments. Energy Convers Manag 2021;230. https://doi.org/10.1016/j.enconman.2020.113793.
[30] İncili V, Karaca Dolgun G, Georgiev A, Keçebaş A, Çetin NS. Performance evaluation of novel photovoltaic and Stirling assisted hybrid micro combined heat and power system. Renew Energy 2022;189:129–38. https://doi.org/10.1016/j.renene.2022.03.030.
[31] Herrando M, Markides CN, Hellgardt K. A UK-based assessment of hybrid PV and solar-thermal systems for domestic heating and power: System performance. Appl Energy 2014;122:288–309. https://doi.org/10.1016/J.APENERGY.2014.01.061.
[32] Mandys F, Chitnis M, Silva SRP. Levelized cost estimates of solar photovoltaic electricity in the United Kingdom until 2035. Patterns 2023;4:100735. https://doi.org/10.1016/j.patter.2023.100735.
[33] Boait PJ, Rylatt RM, Stokes M. Optimisation of consumer benefits from microCombined Heat and Power. Energy Build 2006;38:981–7. https://doi.org/10.1016/J.ENBUILD.2005.11.008.
[34] Balcombe P, Rigby D, Azapagic A. Energy self-sufficiency, grid demand variability and consumer costs: Integrating solar PV, Stirling engine CHP and battery storage. Appl Energy 2015;155:393–408. https://doi.org/10.1016/j.apenergy.2015.06.017.
[35] Chen Y, Yang Z, Wang Y. SOC estimation of lead carbon batteries based on the operating conditions of an energy storage system in a microgrid system. Energies 2019;13:1–25. https://doi.org/10.3390/en13010033.
[36] Wang K, Herrando M, Pantaleo AM, Markides CN. Technoeconomic assessments of hybrid photovoltaic-thermal vs. conventional solar-energy systems: case studies in heat and power provision to sports centres. Appl Energy 2019;254:113657. https://doi.org/10.1016/j.apenergy.2019.113657.
[37] Herrando M, Ramos A, Zabalza I, Markides CN. A comprehensive assessment of alternative absorber-exchanger designs for hybrid PVT-water collectors. Appl Energy 2019;235:1583–602. https://doi.org/10.1016/j.apenergy.2018.11.024.
[38] Herrando M, Ramos A, Zabalza I. Cost competitiveness of a novel PVT-based solar combined heating and power system: influence of economic parameters and financial incentives. Energy Convers Manag 2018;166:758–70. https://doi.org/10.1016/j.enconman.2018.04.005.
[39] Herrando M, Ramos A, Freeman J, Zabalza I, Markides CN. Technoeconomic modelling and optimisation of solar combined heat and power systems based on flat-box PVT collectors for domestic applications. Energy Convers Manag 2018;175:67–85. https://doi.org/10.1016/j.enconman.2018.07.045.
[40] Baxi. Baxi, Ecogen: The Baxi Ecogen Dual Energy System; 2011.
[41] González-Pino I, Pérez-Iribarren E, Campos-Celador A, Terés-Zubiaga J, Las-Heras-Casas J. Modelling and experimental characterization of a Stirling engine-based domestic micro-CHP device. Energy Convers Manag 2020:225. https://doi.org/10.1016/j.enconman.2020.113429.
[42] Obalanlege MA, Xu J, Markides CN, Mahmoudi Y. Techno-economic analysis of a hybrid photovoltaic-thermal solar-assisted heat pump system for domestic hot water and power generation. Renew Energy 2022;196:720–36. https://doi.org/10.1016/j.renene.2022.07.044.
[43] Herrando M, Markides CN. Hybrid PV and solar-thermal systems for domestic heat and power provision in the UK: Techno-economic considerations. Appl Energy 2016;161:512–32. https://doi.org/10.1016/j.apenergy.2015.09.025.
[44] http://web.mit.edu/2.813/www/readings/APPENDIX.pdf.
[45] Cossutta M, Foo DCY, Tan RR. Carbon emission spinch analysis (CEPA) for planning the decarbonization of the UK power sector. Sustain Prod Consum 2021;25:259–70. https://doi.org/10.1016/j.spc.2020.08.013.
[46] Conroy G, Duffy A, Ayompe LM. Economic, energy and GHG emissions performance evaluation of a WhisperGen Mk IV Stirling engine μ-CHP unit in a domestic dwelling. Energy Convers Manag 2014;81:465–74. https://doi.org/10.1016/J.ENCONMAN.2014.02.002.
[47] Herrando M, Simón R, Guedea I, Fueyo N. The challenges of solar hybrid PVT systems in the food processing industry. Appl Therm Eng 2021:184. https://doi.org/10.1016/j.applthermaleng.2020.116235.

[48] Stamford L, Greening B, Azapagic A. Life cycle environmental and economic sustainability of Stirling engine micro-CHP systems. Energy Technol 2018;6: 1119–38. https://doi.org/10.1002/ente.201700854.
[49] Stovesandsolar. Stovesandsolar; 2023.
[50] stovesandsolar. Solax 5.0kW Boost Inverter (model: SL-X1BOOST-5.0T). Stovesandsolar; 2023.
[51] https://www.rateinflation.com/inflation-rate/uk-historical-inflation-rate/ n.d.
[52] Statista. Thermal efficiency of combined cycle gas turbine stations in the United Kingdom (UK) from 2010 to 2021. Stat Res Dep 2023.
[53] Justine Piddington, Simon Nicol, Helen Garrett MC. The Housing Stock of The United Kingdom; 2020.
[54] Milton Keynes Energy Park Dwellings. UK Energy Research Centre Energy Data Centre (UKERC-EDC); 2023.
[55] Energy Saving Trust. Solar Energy Calculator Sizing Guide; 2015.
[56] Williams B. Genopt and trnopt programs; 2023.
[57] Meteonorm Data Base. Meteonorm Data Base; 2023.